Nuclear Instruments and Methods in Physics Research 220 (1984) 561–570
North-Holland, Amsterdam

ELECTRON CLOUD SIZES IN GAS-FILLED DETECTORS

A.J.F. DEN BOGGENDE and C.J. SCHRIJVER

The Astronomical Institute, Space Research Laboratory, Beneluxlaan 21, 3527 HS Utrecht, The Netherlands

Received 2 August 1983

Electron cloud sizes have been calculated for gas mixtures containing Ar, Xe, CO_2, CH_4, and N_2 for drifts through a constant electric field. The transport coefficients w and D/μ are in good agreement with experimental data of various sources for pure gases. Results of measurements, also performed in this work, for $Ar+CO_2$, $Ar+CH_4$, and $Ar+Xe+CO_2$ mixtures are in fair agreement with the calculated cloud sizes.

For a large number of useful gas mixtures calculated electron cloud sizes are presented and discussed, most of which are given for the first time. A suggestion is made for an optimal gas mixture for an X-ray position sensitive proportional counter for medium and low energies.

1. Introduction

Proportional counters have received increasing interest since it was found that these detectors could be used to obtain position information about detected photons or particles. Higher sensitivities were reached by enlarging the gas volume together with increasing the number of wires, which led to the so-called multiwire proportional counters (MWPC) or, especially where particle detection is important, the multiwire drift chambers (MWDC) (e.g. refs. 1,2).

Although most of the developments were stimulated initially in the field of high energy physics, the applicability of these MWPCs in astrophysics soon became clear. The introduction of grazing incidence optical telescopes in the soft X-ray regime required detectors with imaging properties. For this, proportional counters are particularly useful, because of the combined spatial and (limited) spectral resolving power. In these gas-filled detectors the X-ray photons, after entering the detector through an entrance window, produce groups of primary electrons. These electrons will drift, under the influence of an applied electric field, to a read-out system, which is often a part of the total gas volume. Here the number of electrons is increased by gas multiplication, before electronics can handle this information further.

The drift characteristics of the primary electrons in the counter gas are of considerable importance to the position accuracy, which is, apart from other parameters, dependent on the size of the electron cloud when it enters the read-out system.

A mixture of gases is used in proportional counters. Each of the components has a specific function. Often a noble gas constituent (e.g. Ne, Ar, Xe) ensures the desired degree of absorption of the incoming radiation. A quench gas component, being a multi-atomic gas (e.g. CO_2, CH_4), is needed to control the electron avalanche during the gas multiplication. In imaging proportional counters a third requirement is added: the electron cloud size must be matched with the read-out system and the required position resolution. The combination of these three functions makes optimization of the composition of a counter gas mixture rather complex.

We have studied electron cloud sizes for a number of gas mixtures – containing argon, xenon, carbon dioxide and methane – theoretically and experimentally. Later nitrogen was added in the theoretical studies. Our model calculations follow, to a large extent, earlier studies [3,4]. A computer program has been developed in order to calculate the electron cloud sizes (fwhm) as function of the (homogeneous) electric field in the drift space for a given gas composition, temperature and pressure. Required are cross sections for the individual gases for elastic, as well as inelastic scattering, and some atomic data. The diffusion coefficient, the mean drift velocity, and the characteristic energy of the drifting electrons were also determined. We restricted ourselves to electric field strengths below 1000 V/cm, quite common in the drift space of proportional counters.

In order to check the model calculations we performed measurements using a simple counter with a planeparallel configuration.

In the next section the theoretical model used for our calculations is described, following in section 3 by a description of the experimental efforts. In section 4 the experimental and theoretical results are compared, while more results of our model calculations will be presented in section 5 for a number of gas mixtures. Finally, section 6 gives a discussion and the conclusions together with a proposed suitable gas mixture for an imaging

proportional counter for the soft and medium energy X-ray range.

2. Theoretical considerations on cloud size calculations

When a photon is absorbed in the gas mixture in the drift space of a counter a photo-electron is released. This electron ionizes several gas molecules, thus creating a cloud of primary electrons. For photon energies around 2 keV the initial cloud size will be less than approximately 20 μm [5], due to the low mean free path of the photo-electron and of the Auger electrons. For higher energies the range of these electrons introduces an additional (random) error in the position determination.

Once the initial cloud is formed it will drift in the electric field E applied in the drift space. During this process the electrons will diffuse; the mathematical description of this can be deduced using the equation of motion for charged particles in an electric field, together with the equation of continuity, and the relation between the electric field and the mean drift velocity w of the center of the cloud:

$$w = \mu E. \tag{1}$$

Here μ is the mobility of the electrons, a function of the gas composition, pressure and temperature, and the applied electric field. The solution of the resulting differential equations gives the (Gaussian) spatial distribution $n(r,t)$ of the electrons within the cloud after drifting a distance d in t seconds:

$$n(r,t) \propto \exp\left\{\left[(x-t)^2 + y^2 + z^2\right]/4Dt\right\}, \tag{2}$$

where D is the diffusion coefficient. The electric field is applied in the x direction. The cloud size (fwhm) can then be written as:

$$\text{fwhm} = 2.355(2Dt)^{1/2} = 3.330(Dd/w)^{1/2}. \tag{3}$$

The calculation of the fwhm value therefore requires knowledge of the transport coefficients D and w. The coefficients are determined by balancing the energy gain from the field against the energy loss due to elastic and inelastic collisions of the electrons with the gas atoms or molecules [3,4]. The evaluation of the energy distribution function of the electrons within the cloud has been described extensively elsewhere [4]. Only a general outline is given here.

With the mean free path l_e of the electrons between two collisions, and the mean fraction of energy Λ lost in the collisions both dependent on the electron energy ϵ, the energy distribution function $F(\varepsilon)$ can be approximated by:

$$F(\varepsilon) = C(\varepsilon)^{1/2} \times \exp\left[-\int_0^{\varepsilon} \frac{3\Lambda(\varepsilon')\varepsilon'}{\left[eEl_e(\varepsilon')\right]^2 + 3\Lambda(\varepsilon')\varepsilon' kT}\,\mathrm{d}\varepsilon'\right], \tag{4}$$

with C the normalization constant of the distribution, k the Boltzmann constant, and T the absolute temperature. Note that $F(\varepsilon)$ reduces to the well known Maxwell distribution function if the term $[eEl_e(\varepsilon)]^2$ is small compared to $3\Lambda(\varepsilon)\varepsilon kT$ (which describes the effects of thermal motions in the gas on the drifting electrons). The fractional energy loss is given by:

$$\Lambda(\varepsilon) = 2m/M + \sum_h \frac{\varepsilon_h \sigma_h(\varepsilon)}{\varepsilon \sigma_e(\varepsilon)}. \tag{5}$$

The first term on the right hand side gives the mean fractional energy loss due to elastic collisions between an electron with mass m and a gas molecule with mass M. The second term describes the mean fractional energy loss due to inelastic collisions: collisions causing rotational, vibrational and electronic excitations. The excitation energy of the hth rotation or vibration level is represented by ε_h, and σ_h is the cross section corresponding to that level. The momentum transfer cross section (for elastic collisions) is σ_e.

The transport coefficients D and w can be expressed in terms of the energy distribution function $F(\varepsilon)$ [4]:

$$w = \sqrt{\frac{2}{9m}}\,\frac{eE}{N}\int_0^{\infty} \frac{\varepsilon'}{\sigma_e(\varepsilon')}\,\frac{\delta}{\delta\varepsilon'}\left[\frac{F(\varepsilon')}{\sqrt{\varepsilon'}}\right]\mathrm{d}\varepsilon', \tag{6}$$

$$D = \sqrt{\frac{2}{9m}}\,\frac{1}{N}\int_0^{\infty} \frac{\sqrt{\varepsilon'}}{\sigma_e(\varepsilon')} F(\varepsilon')\,\mathrm{d}\varepsilon'. \tag{7}$$

Here N is the number of particles per unit volume, simply related to the total pressure P (in mm Hg) and the absolute temperature T (K) by:

$$N = 2.687 \times 10^{19}(P/760)\,(273/T) \quad \mathrm{cm}^{-3}. \tag{8}$$

In gas mixtures the collision cross section $\sigma_{e,m}$ for a mixture of j gases, each with a partial pressure $\delta_i p$, is given by:

$$\sigma_{e,m} = \sum_{i=1}^{j} \delta_i \sigma_{e,i}. \tag{9}$$

The average fractional energy loss Λ_m per collision in a mixture is given by:

$$\Lambda_m = \sum_{i=1}^{j} (\delta_i \sigma_{e,i} \Lambda_i)/\sigma_{e,m}. \tag{10}$$

If the distribution function $F(\varepsilon)$ for the electrons within the cloud is substituted in the expression for w [eq. (5)] we obtain:

$$w = \sqrt{\frac{2}{9m}}\,\frac{eE}{N}\int_0^{\infty} \frac{\sqrt{\varepsilon'}}{\sigma_e(\varepsilon')} F(\varepsilon') \times \left\{\frac{3\Lambda(\varepsilon')\varepsilon'}{(eE/\sigma_e N)^2 + 3\Lambda(\varepsilon')\varepsilon' kT}\right\}\mathrm{d}\varepsilon'. \tag{11}$$

Comparison of eq. (11) with the expressions for D [eq. (7)], and for $F(\varepsilon)$ [eq. (4)] shows that they are closely

related. for each integration step $F(\varepsilon)\sqrt{\varepsilon}/\sigma_e$ has to be calculated, for which the second term in the integral for w has to be known. The calculation of fwhm [$\sim (D/w)^{1/2}$, eq. (2)] does not require the knowledge of the normalization constant C in eq. (3). This constant is required only for explicitly calculating the values of D and w. It follows from the above arguments that, if the calculated value of w is in agreement with experimental data, D and fwhm are very likely to be correct as well. The drift velocity w and values for D/μ are compared with experimental data for the pure gases in section 4.

Elastic as well as inelastic cross sections for electron–molecule collisions in the pure gases, or the fractional energy loss as a function of the electron energy are needed as basic data. For CH_4 we use the approximation given by Schultz and Gresser [4] rather than that by Palladino and Sadoulet [3], because the first yields a better agreement with experimental results for low electric fields. For N_2 we use the elastic and vibrational cross sections from Engelhardt et al. [11], where cross sections for only two transitions are given. To obtain cross sections for other levels the theory discussed by Gerjuoy and Stein [12] has been applied. Starting with the lowest transitions, higher ones were added until an acceptable agreement was obtained between the calculated and the measured drift velocities (see section 4). The cross sections, as used in our calculations, are summarized in the Appendix.

Cross sections for electronic excitation and for ionization are not incorporated in the model. This requires that the electron energies remain below approximately 4 eV. This condition is almost always met in our calculations for electric fields up to about 1000 V/cm at pressures near 1 atm.

3. Cloud size measurements

In order to obtain appropriate data for a comparison with our calculations electron cloud sizes have been determined experimentally for several gas mixtures characteristic for proportional counters.

3.1. The detector and the X-ray source

A proportional counter in a plane parallel configuration has been used, shown schematically in fig. 1. Its window (3.6 μm Mylar with an aluminium coating of about 10 nm on each side) was supported by a grid to withstand the pressure of the counter gas (approx. 1 atm). In the drift space between window and grid (9.7 mm) an electric field was applied in the range from 30 to 300 V/cm. Field correcting rings ensured homogeneous fields. The grid consisted of a crossed wire mesh (wire diameter of 100 μm), with an optical transmission of 0.25, but with an electron transmission approaching

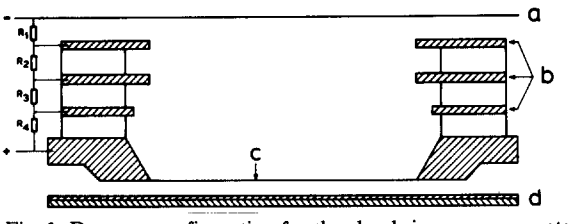

Fig. 1. Detector configuration for the cloud size measurements; a – window, b – field correcting rings, c – grid, d – anode support (glass plate) with anode strips on top (see text).

unity. An anode was placed on a support structure 1.0 mm below the grid. Typical values of the electric field in the gas multiplication space were of the order of 2×10^4 V/cm. Calculations of the field configuration as well as experiments showed, that the field in the drift space was almost unaffected by the presence of the strong gas multiplication field: a reversed field of a few volts in the drift space reduced the counting rate to zero. The anode consisted of 100 μm wide golden strips with a pitch of 200 μm on top of a flat optical glass plate. The signal was tapped from pairs of strips. Measurements were performed on four different positions to enable cross checks on the detector performance.

The detector was connected to a high vacuum (turbopump) system for cleaning and filling. Gas bottles with pure gases and with manufactured standard mixtures were coupled to the system. The amount of oxygen and water vapour in the bottles was less than 5 ppm, that of nitrogen less than 10 ppm.

Radiation from an X-ray source at a distance of about 3.5 m entered the detector through a 500 μm (diameter) hole in a mask placed in front of the window. Carbon K radiation (44.7 Å or 0.277 keV) and Al K radiation (8.34 Å or 1.49 keV) were used. A filter in front of the X-ray source reduced the continuum radiation, favouring the preferred characteristic line radiation.

3.2. The electronic equipment

Signals of the relevant pairs of anode strips as well as that of the grid were fed into separate amplifier chains (charge sensitive preamplifier and shaping amplifier). These chains were individually adjusted to identical amplification. Each chain also contained a low level discriminator, allowing only pulses above a selected minimum level (identical for all chains) to reach a pulse counter. A timer/controller enabled counting during a selected amount of time, followed by a sequential read-out of the counters. The pulse height distribution of the grid signals was measured simultaneously.

3.3. Method of analysis

For each read-out cycle the ratio of the number of counts from each pair of anode strips to the number of

counts from the grid was calculated, together with the mean value and standard deviation for a series of consecutive cycles. As an example the results for two gas mixtures are shown in fig. 2. The mean ratios were used as a measure for the probability of detection of a pulse on a pair of strips, given a detection on the grid.

A detailed analysis of the statistical processes involved yielded a data reduction method. This incorporated statistical fluctuations in the number of primary electrons, their spatial distribution within the cloud (assumed to be Gaussian), the influence of the gas multiplication on the distribution, and the finite beam width. The finite range of the photons in the counter gas has also been incorporated.

Two statistical models were developed, the main distinction being that the number distribution of the electrons above the strips, before multiplication, is taken to be a Gaussian distribution in the first, and a Poisson distribution in the second. We found no significant difference between these two statistical models as far as the central parts of the electron clouds were concerned. Differences between the models were seen in the wings of the distributions, but these were not used for the cloud size determination because of the large uncertainties in average pulse counting rates. It is outside the scope of the present paper to describe the models in full detail; we refer to a report from one of us [13].

A χ^2 analysis was performed to determine the cloud size and its uncertainty. The central position of the electron cloud was a second free parameter. Generally, the pulse counting rates of three pairs of strips were used for the determination of the electron cloud sizes. The covered width of 1200 μm is comparable to or larger than the fwhm of the electron clouds.

The experiments showed, that the spatial distribution of the electrons in the direction perpendicular to the anode strips was in agreement with predicted distributions using the statistical models described above.

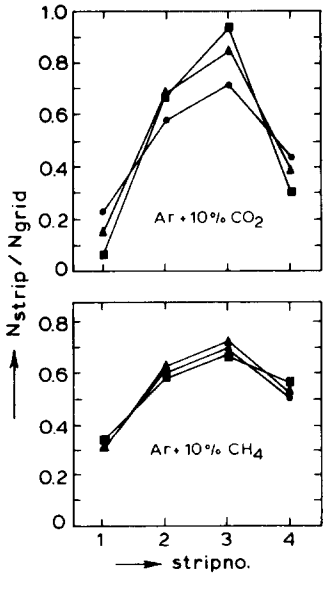

Fig. 2. Ratios of the counting rate of an anode strip and the grid for several strips (1 to 4), for two gas mixtures, and for different electric field strength within the drift space: ● 30 V/cm; ▲ 60 V/cm; ■ 160 V/cm. The uncertainties in the ratios are about equal to the size of the symbols.

4. Comparison of experimental and theoretical results

In this section we compare the experimental values of the transport coefficients reported *in the literature* with our calculations. Also, we shall compare the calculated electron cloud sizes with our experimental results given in section 3.

4.1. Drift velocities and D/μ values in pure gases

Calculated drift velocities and D/μ values have been plotted for pure gases in figs. 3 and 4, together with (averaged) experimental results from various sources in the literature [14–31]. The curves are for 760 mm Hg and 293 K. The agreement between our model and the

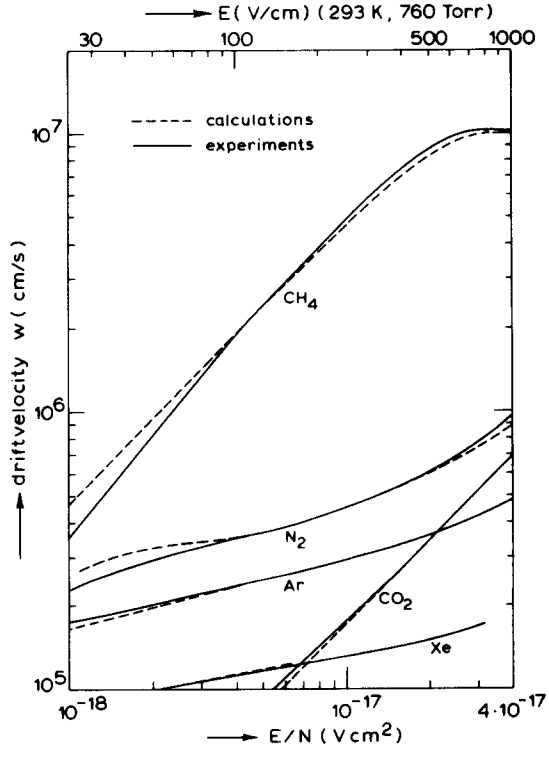

Fig. 3. Drift velocities of electrons in pure gases from our model calculations (---), and experimental values from various sources (—): CH_4 [14–17]; CO_2 [18–21]; N_2 [18,22,23]; Ar [18,22,24]; Xe [21,25].

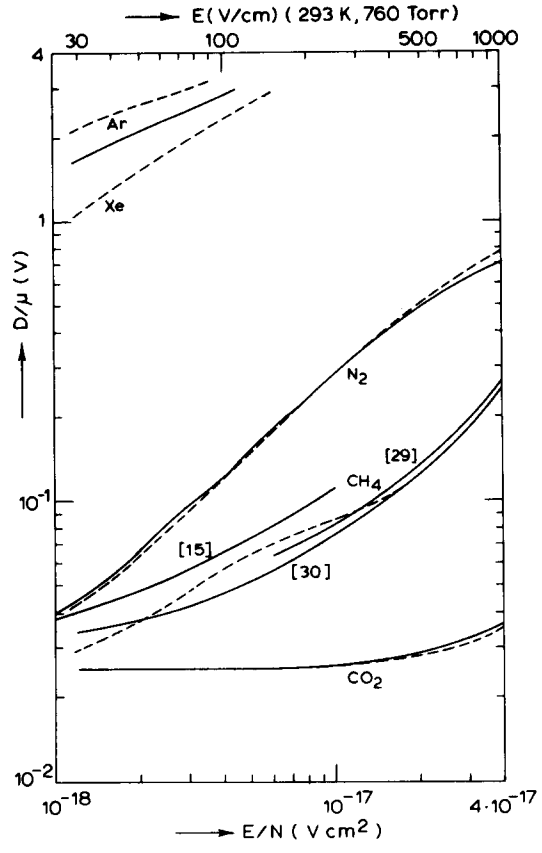

Fig. 4. As fig. 3 but for D/μ. Experimental values: Ar [21,26]; N_2 [27–29]; CH_4 [15,29,30]; CO_2 [28,31]; for Xe no values were found.

experimental results is generally good for the drift velocities (fig. 3). For CH_4 the spread in the experimental results are responsible for a considerable fraction of the deviations. The D/μ (fig. 4) values for N_2 and CO_2 show a good agreement, for CH_4 again the spread in the experimental values is quite large. The present model results in an average value, maybe following the trend indicated by measurements of Cochran and Forrester [29]. The difference between the theoretical and experimental curves for argon is as much as 20%. No experimental D/μ values were found in the literature for xenon. Our results are in a remarkable agreement with the theoretical curve for Kr as given by Lowke and Parker [32].

4.2. Electron cloud sizes in gas mixtures

Results of our electron cloud size measurements are given in table 1. The standard gas mixtures used contained argon, together with either CO_2 or CH_4. In one case xenon was added. The supplier claimed an accuracy of ±1% (abs.) for the quench gas content. No information was available concerning segregation of standard mixtures being in stock up to several years.

Our experimental results for the mixtures are also shown in the figs. 5 and 6, together with results from our cloud size model. In fig. 5a the results are gathered for Ar with (nominally) 5 and 10% CO_2. In order to show the influence of the uncertainty in the CO_2 content of the mixture, the curves for 6%, 9% and 11% CO_2 are shown as well. For the same reason the curve for the mixture of argon and xenon with 4% CO_2 is drawn in fig. 5b, and for argon with 11% CH_4 in fig. 6.

There is a fair agreement for the CO_2 mixtures between the experimental and calculated values for field strengths above 100 V/cm; towards lower field strengths the deviations between the results increase. We also found that the agreement between observed and calculated cloud shapes for the various mixtures at a fixed electric field value became worse for increasing electron cloud sizes. This may indicate that the data reduction program does not describe all the relevant statistics correctly, resulting in a systematic error in the obtained electron cloud sizes. The same effect is probably present in the results for argon with 10% CH_4 (fig. 6): the experimental results are systematically lower than predicted, for cloud sizes much larger than in CO_2 mixtures. This effect may also be responsible for the low cloud size at 300 V/cm in the Ar/Xe/CO_2 mixture (fig. 5b).

We conclude that for electric field strengths in the drift space above 100 V/cm the theoretical predictions agree with experimental results to within approximately 10%. For lower field strengths the experimental values

Table 1
Experimental electron cloud sizes (fwhm in μm) for various gas mixtures and electric fields for 1 cm drift.

Mixture	p [a]	Electric field strength (V/cm)					
		30	60	100	160	200	300
Ar+5% CO_2	800	850±100	690± 70	660±50	650± 50	670± 70	
Ar+10% CO_2	800	820± 70	650± 30	580±20	540± 15	540± 20	490± 30
Ar+50% Xe+5% CO_2	600	835± 90	700± 25	640±25	650± 20	700± 25	800±20
Ar+10% CH_4	800	1270±100	1130±100	1230±60	1230±100	1310±100	1440±100

[a] Total gas pressure in mm Hg; temperature 293 K.

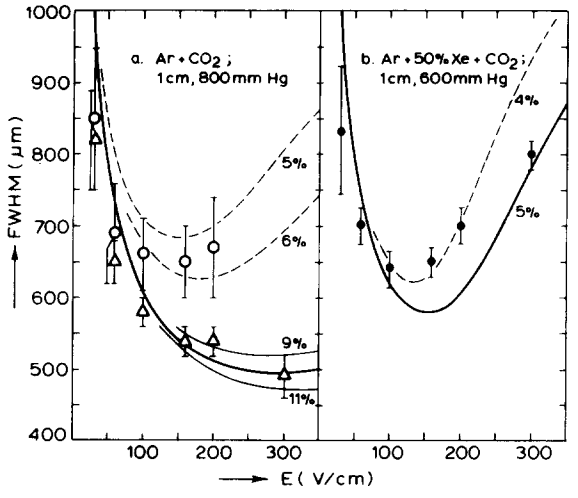

Fig. 5. Our experimental results (see table 1) together with the calculated electron cloud sizes for mixtures containing CO_2 as quenching agent. Indicated is the percentage of CO_2. The uncertainties in the nominal amount of CO_2 are $5\pm1\%$ (○) and $10\pm1\%$ (△).

for the electron cloud sizes are less accurate. However, this region is of less practical importance due to the strong dependence of the cloud sizes on the field strengths.

Contrary to what has been found by Sanford et al. [33] with a plane parallel proportional counter with a resistive disk as anode, we find that adding Xe to Ar mixtures yields smaller cloud sizes, both in theory and in experiment.

We emphasize that in view of the uncertainties in the experimental results (table 1) these values must be considered merely as indicative of the correctness of the theoretical predictions from the model. Obtaining more accurate experimental results requires much more effort, which was not within the scope of the present feasibility study.

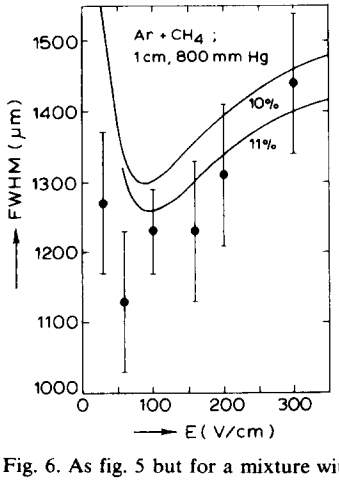

Fig. 6. As fig. 5 but for a mixture with nominally 10% CH_4.

5. Calculated electron cloud sizes for various mixtures

Having established the usefulness of the cloud size model we calculated electron cloud sizes for an additional number of gas mixtures, the field strengths ranging from 50 up to 1000 V/cm. We distinguish: (a) mixtures with only Ar as noble gas constituent, (b) those with only Xe, and (c) those with both Ar and Xe. For the latter group we have, rather arbitrarily, chosen a mixture with 50% Xe.

The results of calculations are depicted in the figs. 7–9. All given cloud sizes are calculated for 760 mm Hg, 293 K and 1 cm path length. We note the typical trend of an initial decrease in cloud size with increasing field strength, the existence of a minimal size, followed by an increase for larger field strengths. The mixtures of Ar and N_2 do not show a minimum below 1000 V/cm.

Fig. 7 shows the electron cloud sizes (fwhm) for mixtures containing Ar and CH_4 and/or N_2. In the CH_4 mixtures the minima are rather narrow, in contrast with those for the CO_2 mixtures (fig. 8). With common amounts of either CH_4 or N_2 in Ar the electron cloud sizes are larger than 1000 μm within the present range of field strengths. The minimum in the curve becomes

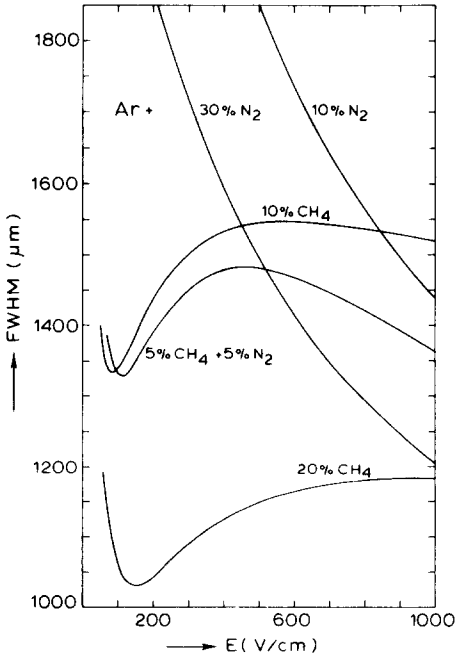

Fig. 7. Calculated electron cloud sizes as function of the electric field strength for 760 mm Hg, 293 K, and 1 cm drift path for Ar mixtures with CH_4 and/or N_2.

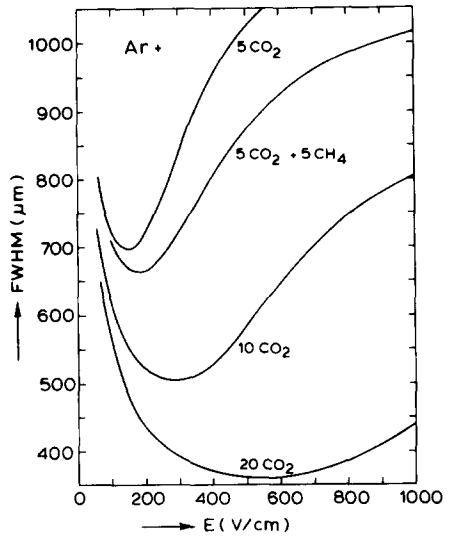

Fig. 8. As fig. 7 but for $Ar + CO_2 (+ CH_4)$ mixtures.

wider and the minimum value lower as the amount of the poly-atomic consituent increases.

The difference between the cloud sizes in the mixtures with 10% CH_4 and 10% N_2 is considerable, whereas replacing half the CH_4 content by N_2 in the 10% CH_4 mixture has little effect. Calculations provide the explanation: drift velocities in $Ar + CH_4$ mixtures are much larger (up to a factor of 10) than in $Ar + N_2$ mixtures for low field strengths, whereas the diffusion coefficients do not differ more than a factor of 3. Therefore, adding CH_4 to an Ar/N_2 mixture causes a strong increase of the drift velocity, whereas it hardly affects the diffusion coefficient, resulting in a smaller cloud.

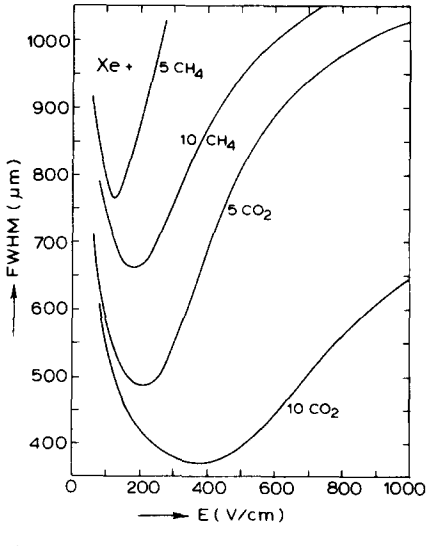

Fig. 9. As fig. 7 but for $Xe + CO_2 (+ CH_4)$ mixtures.

Fig. 8 shows the results for mixtures of Ar and CO_2, one of which has CH_4 added as well. Again the curves show a minimum, and both the minimum value and its width depend on the type and quantity of the gas added: adding CO_2 to a mixture clearly results in a strong decrease of the electron cloud size: for argon mixtures containing only 5% of CO_2 the minimum cloud size is about 700 μm, which is far below the minimum in a mixture with four times as much CH_4 (see fig. 7).

Fig. 9 gives cloud sizes for mixtures in which Xe is the noble gas component. It is seen, as noted in section 4.2, that cloud sizes in mixtures with Xe are smaller than in comparable mixtures without it. Even in a xenon mixture with only 5% CH_4 cloud sizes can lie below 1000 μm. The field strength at minimum cloud size is somewhat larger for xenon mixtures than in argon mixtures. Also the width of the minima is somewhat larger in the xenon mixtures.

The field strength for which the cloud size is minimal depends more strongly on the amount of poly-atomic gas in mixtures of a noble gas with CO_2 than in mixtures with CH_4 or N_2. Also this field strength is larger for mixtures with CO_2 if working with comparable amounts of quench gas (see figs. 7–9).

Fig. 10 shows the dependence of the minimal cloud size on the CO_2 content in $Ar + CO_2$ mixtures as fig. 11 does the for $Ar + Xe + CH_4$ and $Ar + Xe + CO_2$ mixtures with a varying amount of Xe.

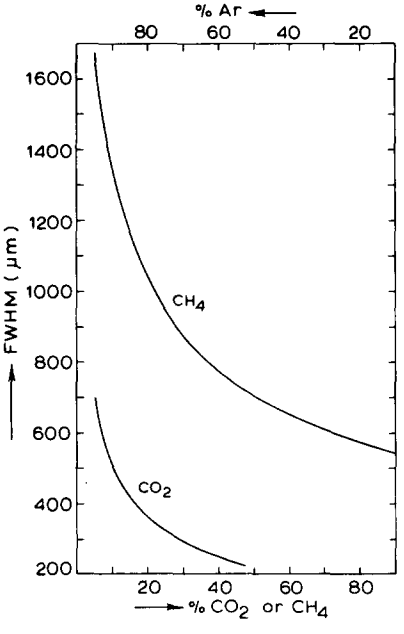

Fig. 10. The calculated minimal electron cloud sizes for $Ar + CO_2$ and $Ar + CH_4$ mixtures as function of the quench gas content.

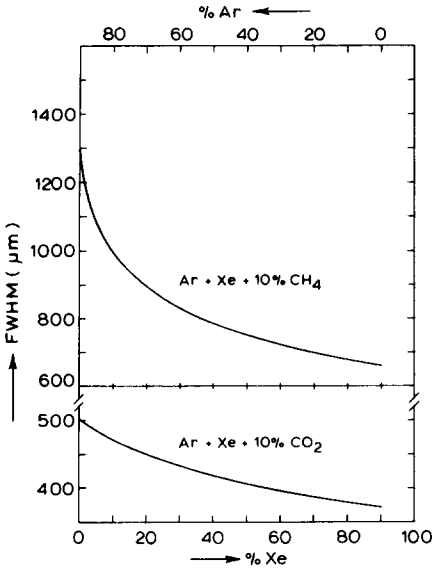

Fig. 11. The calculated minimal electron cloud sizes for Ar + Xe mixtures as function of the Xe content.

6. Conclusions and discussion

We calculated sizes of electron clouds drifting in a homogeneous electric field with strengths below 1000 V/cm for a number of gas mixtures containing Ar, Xe, CO_2, CH_4 and N_2. For pure gases our theoretical results for the transport coefficients D (diffusion) and w (drift velocity) agree well with the experimental values from various sources. For some gas mixtures we have determined the cloud sizes experimentally. These show a fair agreement with our calculations for electric field strengths larger than 50 V/cm. For quite a number of gas mixtures, cloud sizes as function of the electric field strength in the range from 50 to 1000 V/cm are presented graphically (figs. 7–9).

The addition of N_2 to a counter mixture has advantages in gas-filled scintillation detectors (e.g. refs. 34,35). It is not suitable as quenching agent in proportional counters due to its poor absorption power in the wavelength range where Ar and Xe produce their excitation radiation during the gas multiplication process [36]. As can be seen from fig. 7 N_2 produces large electron cloud sizes especially at low field strengths. Note, that about the same cloud sizes are obtained if part of the CH_4 in an Ar + 10%CH_4 mixture is replaced by N_2 (cf. section 5).

For detectors with a read-out system having wire spacings of the order of 2 mm cloud sizes of at least 1000 μm fwhm are required to obtain a constant position resolution over the whole sensitive area. For these detectors mixtures with CH_4 are suitable. However, it is well known that the presence of this molecule produces contamination of anode wires [37,38] (see also ref. 39 for isobutane). Addition of a small amount of Xe will make Xe ions the charge carrier, suppressing the probability of polymerization products that cause deterioration. Addition of a small amount of a non-polymerizing quenching agent with a lower ionization potential than Xe, such as methylal [39] may have the same effect.

For most read-out systems the position resolution and linearity become better as the cloud size decreases, as long as discretisation effects do not occur. This makes CO_2 a favourable component in counter mixtures for those imaging detectors [40], where the read-out system is designed for small cloud sizes. However, CO_2 has a lower quenching ability for the excitation radiation of Ar than CH_4 [36]. This inconvenience can be eliminated to a large extent by adding CH_4 to a mixture of Ar + CO_2. Adding a small amount of Xe to this mixture makes the minimum obtainable cloud size slightly lower without a large increase in high voltage (inherent to the use of Xe) to obtain the same gas gain [41,42]. The added Xe also suppresses the amount of escape radiation and increases the absorption power of the gas in the 4–10 Å (1–3 keV) range as well as below 2.5 Å (above 4.5 keV). This ensures that more photons are absorbed in a thin layer below the window, thus reducing the blurring of images of different wavelengths due to drift-path differences. We therefore conclude, that a promising gas mixture for soft X-ray imaging proportional counters contains Ar with 20–25% Xe and 5%CO_2 + 5%CH_4.

Appendix

Parametrization of the collision cross sections and energy loss functions, used in the calculations:

1) *Argon:*

σ_e as in Schulz and Gresser [4],

$\sigma_h = 0$ for $\epsilon < 11.5$ eV,

$\Lambda = 2m/M = 2.746 \times 10^{-5}$.

2) *Xenon:*

σ_e from Frost and Phelps [6] (also ref. 7) with $l = \ln \epsilon$:

$\epsilon \leqslant 0.2$ eV: $\ln \sigma_e = [(-0.23\, l) - 2.24]l - 56.11$,

$0.2 < \epsilon \leqslant 2.0$ eV: $\ln \sigma_e = (\{[(-0.484\ l) - 1.109]l + 1.11\}l + 1.472)l - 54.5$,
$\epsilon > 2.0$ eV: $= [(-0.724\ l) + 3.105]l - 55.1$.
$\sigma_h = 0$ for $\epsilon < 8.39$ eV.
$\Lambda = 2m/M = 8.356 \times 10^{-6}$.

3) CO_2:
σ_e as in Schulz and Gresser [4].
Λ from Healey and Reed [8]:
$\epsilon \leqslant 0.073$ eV: $\Lambda = 0.0591\ \epsilon^{1/2} + 0.25 \times 10^{-4}$,
$0.073 < \epsilon \leqslant 0.2$ eV: $= [(81.4\ \epsilon - 34.5)\epsilon + 4.86]\epsilon - 0.187$,
$0.2 < \epsilon \leqslant 0.8$ eV: $= [(0.167\ \epsilon - 0.313)\epsilon + 0.176]\epsilon + 0.034$,
$\epsilon < 0.8$ eV: $= \{[(-0.110\ \epsilon + 0.364)\epsilon - 0.321]\epsilon \times 10^{-2} - 0.0229\}\epsilon + 0.0748$.

4) CH_4:
σ_e and σ_h as in Schulz and Gresser [4].
$2m/M = 6.839 \times 10^{-5}$.
$\Lambda = 2m/M + \Sigma\,[\epsilon_h \sigma(\epsilon)/\epsilon\ \sigma_e(\epsilon)]$ for $\epsilon > \epsilon_h$ with:
$\epsilon_1 = 0.08$ eV; $\epsilon_2 = 0.162$ eV; $\epsilon_3 = 0.190$ eV [9].

5) N_2:
σ_e from Table in Huxley and Crompton [10], with $l = \ln \epsilon$:
$\epsilon \leqslant 0.0016$ eV: $\ln \sigma_e = -36.484$,
$0.0016 < \epsilon \leqslant 0.1$ eV: $= \{[(-0.001794\ l) + 0.0239]l + 0.665\}l - 33.665$,
$0.1 < \epsilon \leqslant 0.7$ eV: $= \{[(-0.004278\ l) - 0.316]l - 0.319\}l - 34.637$,
$0.7 < \epsilon \leqslant 1.8$ eV: $= \{[(1.846\ l) + 0.383]l - 0.00585\}l - 34.528$,
$1.8 < \epsilon \leqslant 3.6$ eV: $= \{[(5.952\ l) - 21.919]l + 24.456\}l - 42.036$,
$\epsilon > 3.6$ eV: $= \{[(-0.333\ l) + 2.605]l - 6.454\}l - 29.459$.
$2m/M = 3.9166 \times 10^{-5}$
σ_h: σ_r(rotational) [10–12] and σ_v(vibrational) [10,11]:
$\sigma_r(J, J+2) = 0$, for $J = 0,1$;
$\epsilon_J = 0.249 \times 10^{-3}(4J + 6)$;
$\sigma_r(J, J+2) = 1.179 \times 10^{-17}(J+2)(J+1)(1 - \epsilon_J/\epsilon)^{1/2}/(2J+3)(2J+1)$
for $J = 2,5$ and for $\epsilon > \epsilon_J$;
σ_v with $l = \ln\epsilon$:
$\epsilon \leqslant 0.3$ eV: $\sigma_v = 0$;
$0.3 < \epsilon \leqslant 0.8$ eV: $\ln \sigma_v = \{[(5.367\ l) + 9.519]l - 5.776\}l + 41.220$,
$0.8 < \epsilon \leqslant 2.0$ eV: $= [(9.500\ l) + 2.684]l - 41.918$,
$2.0 < \epsilon \leqslant 2.5$ eV: $= 1.994\ l - 36.877$,
$2.5 < \epsilon \leqslant 3.0$ eV: $= -6.026\ l - 29.528$,
$\epsilon > 3.0$ eV: $= -9.015\ l - 26.244$.
$\Lambda = 2m/M + \{\Sigma[\epsilon_J\ \sigma_r(\epsilon)] + 0.3\ \sigma_v(\epsilon)\}/[\epsilon\ \sigma_e(\epsilon)]$.

We would like to thank all technicians involved in the realization of the instrumentation. We are indebted to H.B. Buurmans for his extensive help throughout the project, and to B.M. Visser for the development of the experimental data reduction method, later complemented by F.G. Cornelis. We acknowledge the stimulating interest of Dr. O.H.W. Siegmund, and Drs. H.F. van Beek, A.C. Brinkman and J.J. van Rooyen for their comments on the draft.

References

[1] G. Charpack, Ann. Rev. Nucl. Sci. 20 (1970) 195.
[2] G. Charpack and F. Sauli, Nucl. Instr. and Meth. 162 (1979) 405.
[3] V. Palladino and B. Sadoulet, Nucl. Instr. and Meth. 128 (1975) 323.
[4] G. Schulz and J. Gresser, Nucl. Instr. and Meth. 151 (1978) 413.
[5] G. Charpack and F. Sauli, Nucl. Instr. and Meth. 152 (1978) 185.
[6] L.S. Frost and A.V. Phelps, Phys. Rev. 136 (1964) A1538.
[7] S.C. Brown, Basic data of plasma physics, 2nd ed. (MIT Press, 1966).
[8] R.H. Healey and J.W. Reed, The behaviour of slow electrons in gases (Amalg. Wireless, Austr., 1947).
[9] G. Herzberg, Molecular spectra and molecular structure III (Van Nostrand, New York, 1966).
[10] L.G.H. Huxley and R.W. Crompton, The diffusion and drift of electrons in gases (Wiley, New York, 1974).
[11] A.G. Engelhardt, A.V. Phelps and C.G. Risk, Phys. Rev. 135 (1964) A1566.

[12] E. Gerjuoy and S. Stein, Phys. Rev. 97 (1955) 1671; 98 (1955) 1848.
[13] C.J. Schrijver, Electron cloud studies in gas mixtures, Internal Report SRL, IVRO 118 (1981).
[14] W.J. Pollock, Trans. Faraday Soc. 64 (1968) 2919.
[15] E.B. Wagner, F.J. Davis and G.S. Hurst, J. Chem. Phys. 47 (1967) 3138.
[16] H. Daum, C.W. Fabjan, S.H. Pordes, M. Franklin, P. Dam and A.F. Rothenberg, Nucl. Instr. and Meth. 152 (1978) 541.
[17] E. Mathieson and M. El Hakeem, Nucl. Instr. and Meth. 159 (1979) 489.
[18] D. Erret, Ph.D. thesis, Purdue Univ. (1951).
[19] W. Riemann, Z. Physik 122 (1944) 216.
[20] M.T. Elford, Austral. J. Phys. 19 (1966) 629.
[21] J.L. Pack, R.E. Voshall and A.V. Phelps, Phys. Rev. 127 (1962) 2084.
[22] J.L. Pack and A.V. Phelps, Phys. Rev. 121 (1961) 798.
[23] J.J. Lowke, Austral. J. Phys. 16 (1963) 115.
[24] J.C. Bowe, Phys. Rev. 117 (1960) 1411.
[25] W.N. English and G.C. Hanna, Can. J. Phys. 31 (1953) 768.
[26] A.G. Engelhardt and A.V. Phelps, Phys. Rev. 133 (1964) A375.
[27] R.W. Crompton and M.T. Elford, Proc. 6th Int. Conf. on Ionisation phenomena in gases (Paris, 1963).
[28] R.W. Warren and J.H. Parker, Phys. Rev. 128 (1962) 2661.
[29] L.W. Cochran and D.W. Forrester, Phys. Rev. 126 (1962) 1785.
[30] C.W. Duncan and I.C. Walker, J. Chem. Soc. Trans. Far. II 68 (1972) 1514.
[31] J.A. Rees, Austral. J. Phys. 17 (1964) 462.
[32] J.J. Lowke and J.H. Parker, Phys. Rev. 181 (1969) 302.
[33] P.W. Sanford, I.M. Mason, K. Dimmock and J.C. Ives, IEEE Trans. Nucl. Sci. NS-26 (1979) 169.
[34] O.H.W. Siegmund, Ph.D. thesis, Univ. of London (1981); O. Siegmund, P. Sanford, I. Mason, L. Culhane, S. Kellock and R. Cockshott, IEEE Trans. Nucl. Sci. NS-28 (1981) 478.
[35] G. Charpack, S. Majewski and F. Sauli, Nucl. Instr. and Meth. 126 (1975) 381; IEEE Trans. Nucl. Sci. NS-23 (1976) 202.
[36] P.J. Nawrochi and R. Papa, Atmospheric processes (Prentice Hall, 1962).
[37] P.W. Sanford and J.L. Culhane, Proc. 2nd Symp. on Low energy X-ray and gamma sources and applications, ORNL-IIC-10 (1967) p. 376.
[38] A.J.F. den Boggende, A.C. Brinkman and W. de Graaff, J. Sci. Instr. (J. Phys. E) 2 (1969) 701.
[39] P. Rice-Evans, Spark, streamer, proportional and drift chambers (Richelieu Press, London, 1974) ch. 7.4.
[40] J.A.M. Bleeker, H. Huizinga, A.J.F. den Boggende and A.C. Brinkman, IEEE Trans. Nucl. Sci. NS-27 (1980) 176.
[41] R.Z. Fuzesy, J. Jaros, L. Kaufman, J. Marriner, S. Parker and V. Perez-Mendes, Nucl. Instr. and Meth. 100 (1972) 267.
[42] R.S. Wolff, Nucl. Instr. and Meth. 115 (1974) 461.